

RSC Advances



This is an *Accepted Manuscript*, which has been through the Royal Society of Chemistry peer review process and has been accepted for publication.

Accepted Manuscripts are published online shortly after acceptance, before technical editing, formatting and proof reading. Using this free service, authors can make their results available to the community, in citable form, before we publish the edited article. This *Accepted Manuscript* will be replaced by the edited, formatted and paginated article as soon as this is available.

You can find more information about *Accepted Manuscripts* in the [Information for Authors](#).

Please note that technical editing may introduce minor changes to the text and/or graphics, which may alter content. The journal's standard [Terms & Conditions](#) and the [Ethical guidelines](#) still apply. In no event shall the Royal Society of Chemistry be held responsible for any errors or omissions in this *Accepted Manuscript* or any consequences arising from the use of any information it contains.

Ultraviolet emission of amorphous SiO_{2+x} nanowires with connected bead-chain morphology

Hui Cao, Yin Zhang and Renchao Che*

Advanced Materials Laboratory and Department of Materials Science,

Fudan University, Shanghai 200438, P. R. China.

Abstract

SiO_{2+x} nanowires composed of multi-beads with novel chain morphology fabricated on an Au-coated silicon substrate were prepared via a chemical vapor deposition (CVD) technique. The morphology and microstructure of nanowires were characterized by scanning electron microscopy (SEM), transmission electron microscopy (TEM), selective area electron diffraction (SAED) and Fourier transform infrared spectroscopy (FTIR). The results showed that the morphology of SiO_{2+x} could be well tuned by changing substrate temperature and deposition condition. Growth process of SiO_{2+x} nanowires was investigated by changing the substrate temperature from 400 °C to 1088 °C and the deposition time from 15 min to 60 min. Hence, a 'dissolution-saturation-precipitation' growth model suitable for the SiO_{2+x} nanowires was proposed. Electron diffraction analysis showed that the nanowires had an amorphous phase structure. The SiO_{2+x} nanowires emitted ultraviolet light with wavelengths of 308, 327 and 345 nm, respectively, which could be attributed to oxygen-rich in the nanowires.

1 Introduction

In the past few years, One-dimensional (1D) nanostructures such as nanowires and nanotubes have attracted many attentions, for which give an impetus to fabricate new kinds of nanodevices in the application fields of electronics, optics and photonics.¹⁻⁴ Intensive researches have focused on Si-based 1D nanomaterials such as SiO_x nanowires and blue photoluminescence of Si-based nanomaterials has been widely reported.⁵⁻⁷ It has been proposed that blue or blue-green light emission of SiO_x nanowires may be related to oxygen vacancies formed in the nanowires, that is, the ratio of Si to O is lower than 2.0.^{6,8} In addition, Yang et al. have observed an ultraviolet photoluminescence emission of ~370 nm in Si oxide and nanostructures, which originates in the '-SiO₃' group.⁹ Xiao et al. have synthesized SiO₂ nanowire arrays with a strong ultraviolet emission band centered at 385 nm and a relatively weaker ultraviolet emission one at 298 nm.¹⁰ However, the research based on the strategy of morphological adjustment for tuning the ultraviolet photoluminescence performance of SiO_x nanowires is still in lack.

Among various SiO_x morphologies, nanowire is the main one which has been successfully fabricated via many routes, such as chemical vapor deposition,^{10,11} laser ablation,¹² thermal evaporation,^{13,14} hydrothermal synthesis,¹⁵ etc. Other morphologies, such as nanobelts,¹⁶ nanotubes,¹⁷ nanolantorns¹³ or nanocakes¹⁴ have also been successfully synthesized.

According to a conventional model of vapor-liquid-solid (VLS) growth,¹⁸ catalyst alloys could be melted into a liquid state to serve as a solvent for effectively absorbing reactants only under elevated temperature. Among the metal catalysts, Au is preferred to be used for SiO_x nanowires growth, as it has low eutectic temperature with silicon (T_e≈363 °C).^{6,14} Other metal catalysts, such as Sn,¹¹ Fe,¹⁹ Ge²⁰ and Ni²¹ have been reported for the growth of SiO_x nanomaterials. Except for VLS mechanism, solid-liquid-solid (SLS) mechanism is also proposed by Wang et al.²²

In this work, a novel type of SiO_{2+x} nanowires with connected bead-chain morphology were successfully fabricated via CVD method by using Au as the catalyst. As far as we know, this morphology has not been reported. Three ultraviolet luminescence peaks of SiO_{2+x} located at 308, 327 and 345 nm, which were different from the

previously reported values of light wavelengths. The Si-based nanowires with connected bead-chain morphology may be potential in applications such as information storage and faster laser typing devices.

2 Experimental

Silicon (100) wafers were used as the source and substrate for the growth of SiO_{2+x} nanowires. The wafer was cleaned by a standard treatment in piranha solution (30% H_2O_2 /20% H_2SO_4),⁶ then rinsed with de-ionized water and acetone, respectively. Then, a thin layer of gold (~15 nm) was sputtered on silicon wafer to serve as a metal catalyst.

In our experiment, Au-catalyzed SiO_{2+x} nanowires were deposited on silicon (100) wafers by atmospheric pressure chemical vapor deposition (CVD). The silicon pieces were placed in the ceramic boat positioned downstream in the inner tube along the direction of gas flow. Different distance between the substrate and the heating center resulted in different growth temperatures due to the natural temperature gradient. The SiO_{2+x} nanowires were grown in a horizontal tube furnace, where temperature and reaction time were tuned and therefore the morphologies of the nanowires could be controlled. During the whole experiment, the mechanical pump worked to evacuate the remaining gas. The silicon pieces were heated from room temperature to 1400°C with the heating rate of 10°C/min and held at this temperature for a certain time (15 min, 30 min and 60 min). During the constant temperature stage, argon gas flow was introduced through the tube at flow rate of 40 sccm. Then the power generator was switched off, allowing the furnace to cool down to room temperature.

The size and morphology of the samples were characterized by a field emission scanning microscope (Hitachi-4800) operated at a working voltage of 1.0-3.0 kV. The diameters of the nanowires were measured by FESEM software and 50 random samples were used for the statistical analysis. Energy-dispersive X-ray spectroscopy (EDX, Bruker Quantax) attached to S-4800 was used to determine the composite composition (the accelerator voltage was 20 kV), the value of which was averaged from ten tests of the investigated sample. TEM analysis was carried out on JEM-2100F (JEOL, 200 kV) field emission microscope equipped with a Gatan Ultrascan CCD camera and EDX (Oxford) detector. For TEM measurement, the as-prepared sample was ultrasonicated in ethanol, and then a drop of the suspension was placed on a carbon-coated copper grid.

Fourier transform infrared spectroscopy (FTIR) spectra were recorded on Nicolet Magna-470 spectrometer (in the range 3000-400 cm^{-1}) using the composite milling with KBr in the mass ratio of 1:20 and pressing into disk. Photoluminescence (PL) measurements were performed on a Shimadzu RF-5301PC type spectrophotometer with a Xe lamp as the excitation light source, as photoluminescence intensity would also depend on the excitation wavelength and 280 nm was chosen as the excitation wavelength at room temperature.

3 Results and discussion

3.1 Processing parameters of chemical vapor deposition

It is believed that the controllable growth of SiO_x nanowires is a complex procedure, therefore, the key parameters such as substrate temperature and deposition condition are carefully examined.

3.1.1 Substrate temperature

Among the various parameters affecting the morphology of nanofibers, the substrate temperature is one of the most effective factors governing the nanowires' growth process. Basically, substrate temperature determines surface diffusion length and the amount of adatoms condensation on the surface.²³ To study the effect of substrate temperature on the growth process, several silicon substrates were supported by a ceramic boat side by side in different temperature zones, respectively.

SEM images of SiO_{2+x} nanowires grown on silicon wafers with Au as a catalyst at a temperature ranging from

400 °C to 1088 °C were shown in Fig. 1. It was interesting to find that as the temperature reached up to be more than a critical temperature of 920 °C, the SiO_{2+x} nanowires with novel bead-chain morphology were obtained. As the temperature reduced to 400 °C, the nanowires with bead-chain morphology were replaced by a lot of nanowires with some nanoparticles (Fig. 1g and 1h), and the size distributions were shown in Fig. 1A-G, indicating that reaction temperature effectively changed the product morphology. The higher substrate temperature, the larger diffusion coefficient of the silicon and the easier migration of silicon atoms into gold particles to form Au-Si alloy, furthermore, silicon oxide particle deposited from the supersaturated droplet. That is, the diameter of sample became larger with increasing the substrate temperature. The scheme of products grown under different temperature of the wafers was shown in Fig. S1.

The chemical composition of nanowires was investigated by EDX. Fig. 2a represented a typical EDX spectrum corresponding to the nanowires with connected bead-chain morphology (Fig. 1a), which consisted of silicon and oxygen and further quantitative analysis showed that the ratio of oxygen to silicon was 2.15 ± 0.03 , a little higher than 2.0 of the standard SiO_2 . That is, the as-prepared nanowires were silicon oxide with oxygen-rich composition. The source of the excess oxygen might come from residual oxygen in the furnace or the impurity from argon gas.^{24,25} Fig. 2b was a typical EDX spectrum corresponding to the nanowires with some particles (Fig. 1g), which was composed of silicon, oxygen and Au coming from the catalyst. Quantitative EDX analysis also indicated that the nanowires were oxygen-rich silicon oxide on average. Fig. 2c and Fig. 2d were EDX mapping scanning spectra of the nanowires acquired at 1088 °C and 400 °C, respectively. It was difficult to observe Au particle in Fig. 2c as the vapor of Au formed and the amount of Au particles became scarce through the whole nanowire under such a high temperature (~1088 °C). Fig. 2d showed that the element distributions of silicon, oxygen and Au were relatively even. It should be mentioned that our EDX data were acquired from a large region including thousands of nanowires, which were quantitatively meaningful.

3.1.2 Deposition condition

Longer deposition time favored the formation of Au-Si alloy with larger size. When the alloy adsorbed the activated silicon ions and oxygen molecules from the gas phase to some extent, supersaturated droplets appeared, thus, SiO_{2+x} nanowires deposited on the wafer. It was reported that the diameter of the nanowires depended on the initial size of Au-Si alloy,²⁶ thus, as shown in Fig. 3, the diameter of the nanowires with bead-chain morphology increased with the deposition time prolonged (from 15min to 60min).

3.2 Growth mechanism of SiO_{2+x} nanowires

SiO_{2+x} nanowires were synthesized using Au as a catalyst. The silicon wafer was the single source for Si supply during the growth process of SiO_{2+x} nanowires. Oxygen might come from the residual oxygen in the furnace or the impurity from argon gas. Oxygen molecules were very active and were easily to react with silicon ions to form silica oxide under high temperature (above ~ 400 °C).

In this work, as temperature reached ~ 400 °C, SiO_{2+x} nanowires were formed using Au (melting point, 1064°C) as the catalyst for the low eutectic temperature (363°C) of the Au-Si alloy. However, as the size of Au nanoparticle decreased to be within nanometer range, its melting point remarkably reduced to several hundred degrees, which located inside our reaction temperature. When the reaction temperature was higher than the melting point of Au nanoparticle of our specific reaction system, Au particles became melting and started to transform to droplets and reacted with silicon to form Au-Si alloy onto the surface of silicon substrate, which adsorbed activated oxygen molecules and silicon ions from the transported gas phase.

It was possible that an incontinuous growth model was a suitable description for the bead-chain morphology. Au-Si alloys as the nucleation sites induced an initiation of the growth of silicon oxide particles from the

supersaturated droplets, furthermore, silicon ions and oxygen molecules adsorbed on the surface of silicon oxide particle to form another particle. The growth of the silicon oxide particles was discontinuous and SiO_{2+x} nanowires were obtained with repeating the above process. Only under a certain temperature of 920 °C, which was high enough to provide kinetics energy for the whole process: the melting of Si, the formation of Si-Au alloy, and the completion of discontinuous growth.

It should be pointed out that the catalyst might not be at the top the nanowire. Yu et al. reported that catalyst was usually visible in the middle part, instead of being attached to the end of the SiONWs .³ Meng et al. indicated that no nanoparticles were observed on either end of the nanowires.⁸ Zhang et al. also reported that no nanoparticles attached at the tip among all the nanowires.¹¹ In this work, it was suggested that at early stage Au rested at the base of the nanowires on the substrate. When the temperature of the furnace was raised up higher than 700 °C, the vapor of Au formed and the amount of Au particles became scarce through the whole nanowire, thus, it was difficult to observe Au on nanowires with bead-chain morphology by SEM and TEM. It should be mentioned that there were still a few Au particles migrated and stopped in the middle of the nanowires (as shown in Figure 1h) as the temperature ranged from 400 °C to 700 °C. The reason could be that under the low temperature, Au did not volatilize fully.

The normal VLS mechanism was not suitable to explain the growth of SiO_{2+x} nanowires because no Au nanoparticles existed at the tip of the nanowires. Therefore, a 'dissolution-saturation-precipitation' growth model suitable for the SiO_{2+x} nanowires was proposed. The higher substrate temperature, the larger diffusion coefficient of the silicon and the easier migration of silicon atoms into gold particles to form Au-Si alloy. Higher reaction temperatures and longer deposition time favored the formation of Au-Si alloy with larger size. As the diameter of the nanowires depended on the initial size of Au-Si alloy,²⁶ it was indicated that the diameter of SiO_{2+x} nanowires became larger with increasing substrate temperature and deposition time (Fig. 4).

3.3 Structural studies of SiO_{2+x} nanowires

Detailed structural and chemical analysis of individual nanowire with bead-chain morphology was carried out using transmission electron microscopy (TEM). Fig. 5a was a TEM image of a typical obtained SiO_{2+x} nanowire with bead-chain morphology. The highly diffusive ring pattern in the corresponding selected area electron diffraction (SAED) patterns indicated that the obtained SiO_{2+x} nanowire was amorphous phase (the insert of Fig. 5a). SiO_{2+x} nanowire grown at lower temperature (~ 400 °C) was of a completely amorphous state, too (as shown in Fig. S2).

Fig. 5b was the EDX spectrum of the nanowire which showed that the nanowire was composed of silicon and oxygen elements. Meanwhile, the elements of Cu and carbon came from TEM grid. Quantitative analysis showed that the ratio of oxygen to silicon was 2.16 ± 0.05 , which agreed with the result of SEM-EDX. To strengthen the claim that oxygen was in excess inside the nanowires, EDX on a quartz sample with high purity was performed as a reference and the result showed that the ratio of O to Si was 2.02 ± 0.03 (as shown in Fig. S3). Fig. 5d and 5e showed that the element distributions of oxygen and silicon were uniform.

The FTIR spectrum of the synthesized SiO_{2+x} nanowires was shown in Fig. 6. It showed the Si-O-Si bond rocking vibrational mode appeared at 472 cm^{-1} , the O-Si-O bond bending mode appeared at 804 cm^{-1} and the strongest absorption peak located at 1105 cm^{-1} .²⁷ It was reported that the appearance of 1130 cm^{-1} was attributed to the highly disordered structure of thin SiO_2/Si nanowires.²⁷ The above results indicated that there was no trace of a crystalline phase in our SiO_{2+x} nanowires. Furthermore, the EDX analysis showed the oxygen of SiO_{2+x} nanowires was non-stoichiometric. Thus, the shift from 1130 cm^{-1} to 1105 cm^{-1} could be attributed to the effect of the oxygen excess. In this work, the strongest absorption peak at 1105 cm^{-1} was considered due to the disordered structure of amorphous SiO_{2+x} nanowires. In addition, FTIR spectrum of the SiO_{2+x} nanowires prepared at lower temperature

(~ 400°C) was shown in Fig. S4. And there was no obvious difference for FTIR spectra from samples grown at different temperatures.

3.4 Optical property

Fig. 7 showed a typical PL spectrum of SiO_{2+x} nanowires with connected bead-chain morphology at room temperature. Ultraviolet intensive peaks can be deconvoluted in three bands centered at 327 nm (3.79 eV) together with two shoulder peaks at 308 nm (4.03 eV) and 345 nm (3.60 eV). Yang et al. observed an ultraviolet photoluminescence emission of ~370 nm in Si oxide and nanostructures, which originated in the '-SiO₃' group.⁹ Xiao et al. synthesized SiO₂ nanowire array with a strong ultraviolet emission band centered at 385 nm and a relatively weaker ultraviolet emission one at 298 nm.¹⁰ Qin et al. demonstrated that some oxygen excess defects might be responsible for the UV light emission around 350 nm wavelengths in the silicon oxide.²⁸ Sun et al. observed UV emissions from thermally oxide porous silicon, which was supposed to be related to oxygen excess defects.²⁹ Wang et al. and Meng et al. also proposed that blue or blue-green light emission of SiO_x nanowires might be related to oxygen vacancies formed in the nanowires, that is, the ratio of Si to O was lower than 2.0.^{6,8} Maybe there was a relationship between optical property and the ratio of Si to O. As it was confirmed in the above EDX result that the fabricated nanowires were silicon oxide with oxygen-rich region, it was considered that ultraviolet intensive peaks around 308, 327 and 345 nm were related to the excess oxygen in the nanowires.

4 Conclusions

In summary, an amorphous SiO_{2+x} nanowires with connected bead-chain morphology were successfully synthesized by using a substrate wafer as the silicon source via CVD reaction. The diameter of SiO_{2+x} nanowires became larger with higher deposition temperature and longer deposition time. A 'dissolution-saturation-precipitation' growth model suitable for the SiO_{2+x} nanowires was proposed. Photoluminescence measurements indicated that there were three emission peaks at 308, 327 and 345 nm (corresponding to around 4.03, 3.79 and 3.60 eV), respectively.

Acknowledgments

This work was supported by the Ministry of Science and Technology of China (973 Project Nos. 2013CB932901 and 2009CB930803), the National Natural Foundation of China (Nos. 51172047, 50872145 and 51102050) and NSAF (U1330118), and the This project was sponsored by Shanghai Pujiang Program and 'Shu Guang' project of Shanghai Municipal Education Commission and Shanghai Education Development Foundation (09SG01).

References

- 1 Y. Cui and C. M. Lieber, *Science*, 2001, **291**, 851.
- 2 Y. Cui, X. F. Duan, J. T. Hu and C. M. Lieber, *J. Phys. Chem. B*, 2000, **104**, 5213.
- 3 D. P. Yu, Q. L. Hang, Y. Ding, H. Z. Zhang, Z. G. Bai, J. J. Wang, Y. H. Zou, W. Qian, G. C. Xiong and S. Q. Feng, *Appl. Phys. Lett.*, 1998, **73**, 3076.
- 4 L. M. Tong, J. Y. Lou, R. R. Gattass, S. L. He, X. W. Chen, L. Liu and E. Mazur, *Nano Lett.*, 2005, **5**, 259.
- 5 S. Jang, Y. Lee, S. Kim, J. Seo and D. Kim, *Mater. Lett.*, 2011, **65**, 2979.
- 6 Y. W. Wang, C. H. Liang, G. W. Meng, X. S. Peng and L. D. Zhang, *J. Mater. Chem.*, 2002, **12**, 651.
- 7 P. Lv, Z. Q. Zhang, X. T. Wang, X. L. Hou and Q. F. Guan, *Rsc Adv.*, 2013, **3**, 17998.
- 8 G. W. Meng, X. S. Peng, Y. W. Wang, C. Z. Wang, X. F. Wang and L. D. Zhang, *Appl. Phys. a-Mater.*, 2003, **76**, 119.

- 9 X. Yang, X. L. Wu, S. H. Li, H. Li, T. Qiu, Y. M. Yang, P. K. Chu and G. G. Siu, *Appl. Phys. Lett.*, 2005, **86**, 201906.
- 10 Z. D. Xiao, L. D. Zhang, G. W. Meng, X. K. Tian, H. B. Zeng and M. Fang, *J. Phys. Chem. B*, 2006, **110**, 15724.
- 11 J. Zhang, B. L. Xu, Y. D. Yang, F. H. Jiang, J. P. Li, X. C. Wang and S. Wang, *J. Non-Cryst. Solid*, 2006, **352**, 2859.
- 12 I. Aharonovich, S. Tamir and Y. Lifshitz, *Nanotechnology*, 2008, **19**, 065608.
- 13 P. Wu, X. Q. Zou, L. F. Chi, Q. Li and T. Xiao, *Nanotechnology*, 2007, **18**, 125601.
- 14 M. S. Al-Ruqeishi, R. M. Nor, Y. M. Amin and K. Al-Azri, *Silicon*, 2011, **3**, 145.
- 15 L. W. Lin, Y. H. Tang, X. X. Li, L. Z. Pei, Y. Zhang and C. Guo, *J. Appl. Phys.*, 2007, **101**, 014314.
- 16 Z. Y. Zhang, X. L. Wu, L. L. Xu, J. C. Shen, G. G. Siu and P. K. Chu, *J. Chem. Phys.*, 2008, **129**, 164702.
- 17 M. Zhou, J. Y. Zhou, R. S. Li and E. Q. Xie, *Nanoscale Res. Lett.*, 2010, **5**, 279.
- 18 R. S. Wagner and W. C. Ellis, *Appl. Phys. Lett.*, 1964, **4**, 89.
- 19 Y. J. Chen, J. B. Li and J. H. Dai, *Chem. Phys. Lett.*, 2001, **344**, 450.
- 20 T. X. Nie, Z. G. Chen, Y. Q. Wu, J. H. Lin, J. Z. Zhang, Y. L. Fan, X. J. Yang, Z. M. Jiang and J. Zou, *J. Alloy Compd.*, 2011, **509**, 3978.
- 21 Z. M. Yang, Z. Yu, H. Chen, Z. F. Jiao, Y. Jin, Y. He, M. Gong and X. S. Sun, *J. Non-Cryst. Solids*, 2008, **354**, 1731.
- 22 C. Y. Wang, L. H. Chan, D. Q. Xiao, T. C. Lin and H. C. Shih, *J. Vac. Sci. Technol. B*, 2006, **24**, 613.
- 23 M. Rajabi, R. S. Dariani and A. I. Zad, *Mater. Sci. Semicond. Process.*, 2013, **16**, 171.
- 24 Z. W. Pan, Z. R. Dai, C. Ma and Z. L. Wang, *J. Am. Chem. Soc.*, 2002, **124**, 1817.
- 25 R. Z. Ma and Y. Bando, *Chem. Phys. Lett.*, 2003, **377**, 177.
- 26 Y. Cui, L. J. Lauhon, M. S. Gudiksen, J. F. Wang and C. M. Lieber, *Appl. Phys. Lett.*, 2001, **78**, 2214.
- 27 T. Noda, H. Suzuki, H. Araki, W. Yang, Y. Shi and A. Tosa, *Appl. Surf. Sci.*, 2005, **241**, 231.
- 28 G. G. Qin, J. Lin, J. Q. Duan and G. Q. Yao, *Appl. Phys. Lett.*, 1996, **69**, 1689.
- 29 H. B. Song, Z. W. Li, H. Chen, Z. F. Jiao, Z. Yu, Y. Jin, Z. M. Yang, M. Gong and X. S. Sun, *Appl. Surf. Sci.* 2008, **254**, 5655.

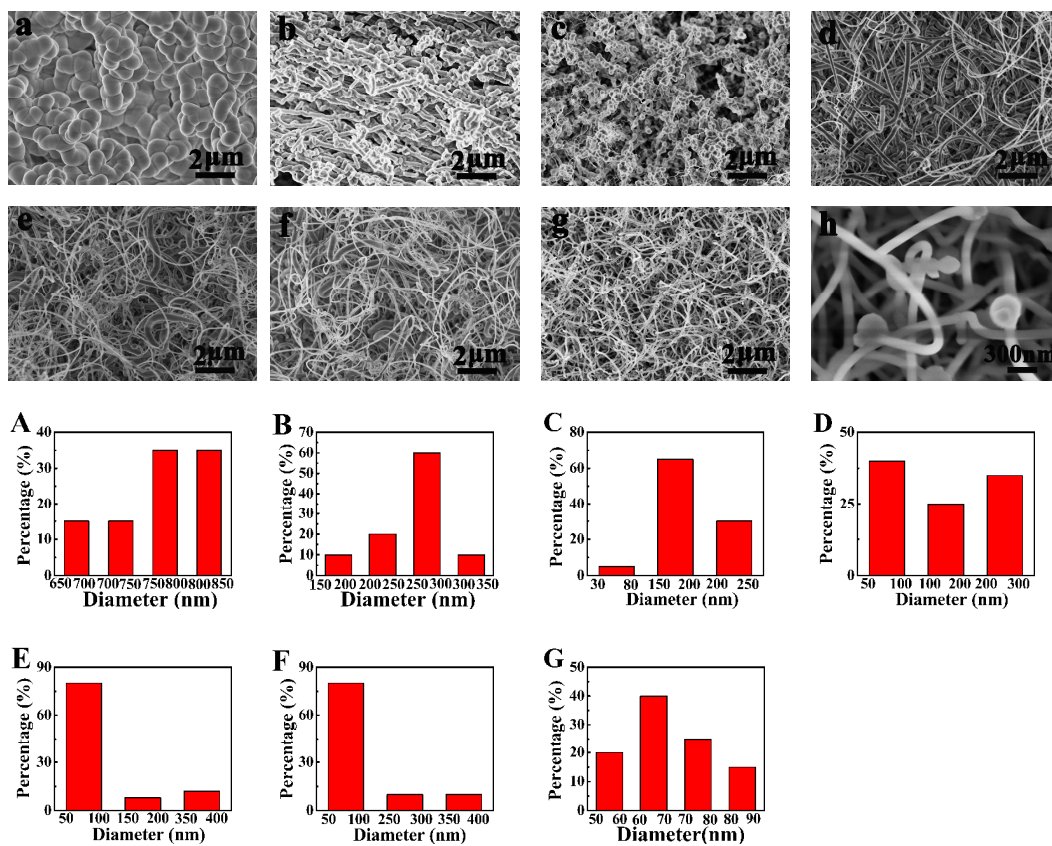


Fig.1 SEM images of SiO_{2+x} prepared at different temperatures, (a) 1088°C, (b) 920°C, (c) 800°C, (d) 700°C, (e) 600°C, (f) 500°C and (g) 400°C. Image of (h) was the enhanced image of (g). Size histograms of SiO_{2+x} prepared at the corresponding temperatures were (A), (B), (C), (D), (E), (F) and (G), respectively. The deposition time was set as 30 min and the thickness of Au was ~15 nm.

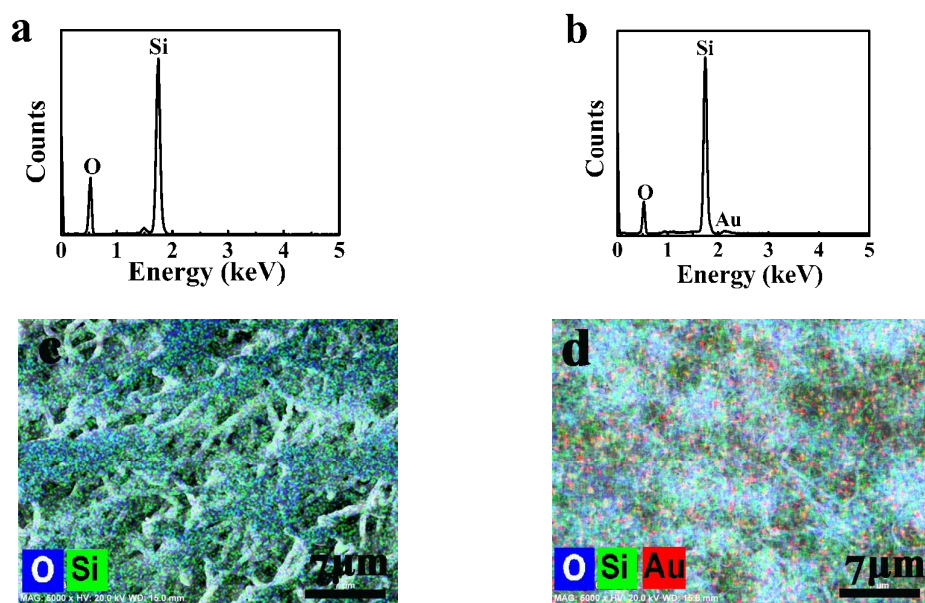


Fig.2 EDX spectra of the nanowires at different temperatures, (a) 1088°C, (b) 400°C. The corresponding EDX mapping scanning spectra of the nanowires at different temperatures, (c) 1088°C, (d) 400°C. For mapping scanning spectra, the color of blue, green and red represented the distributions of oxygen, silicon and gold, respectively. The deposition time was set as 30 min.

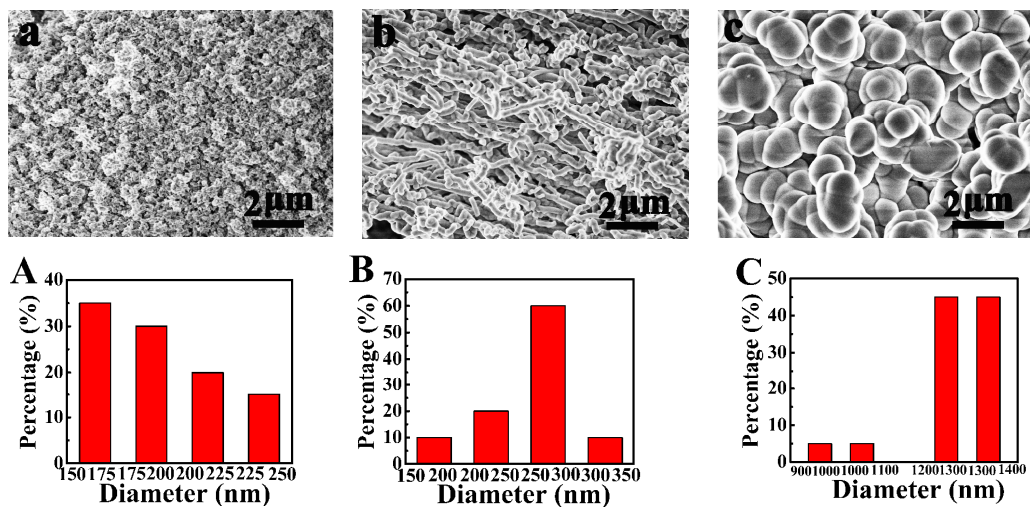


Fig. 3 SEM images of SiO_{2+x} prepared with different deposition time, (a) 15 min, (b) 30 min and (c) 60 min. Size histograms of SiO_{2+x} prepared with different deposition time (A) 15 min, (B) 30 min and (C) 60 min. The temperature was set as ~ 920 °C.

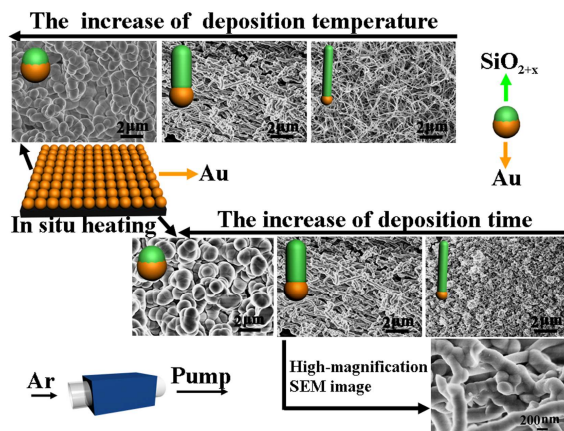


Fig.4 Scheme of a 'dissolution-saturation-precipitation' growth model for SiO_{2+x} nanowires.

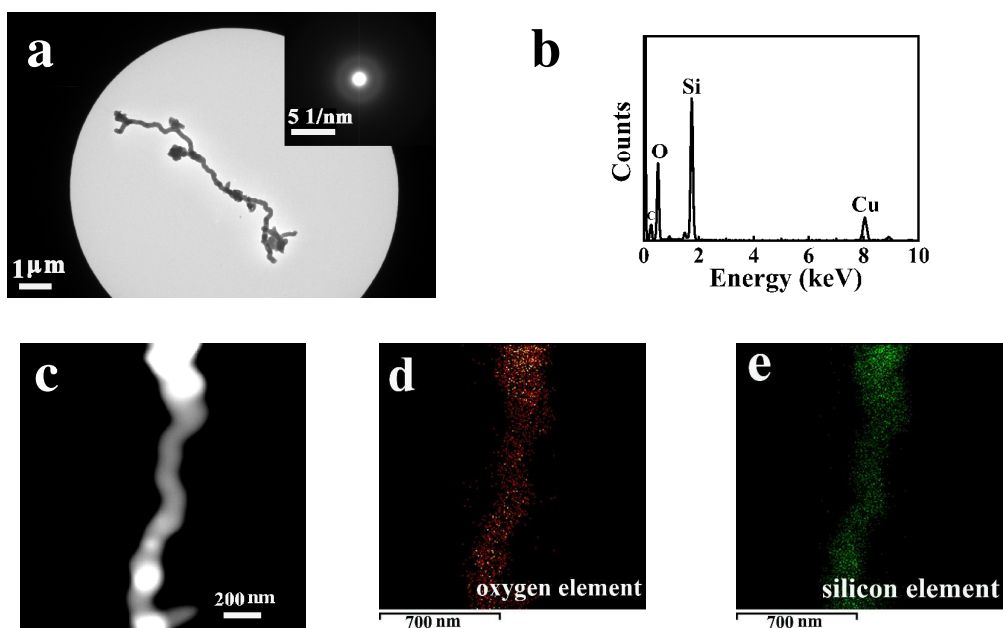


Fig.5 TEM image of (a) SiO_{2+x} , the insert was the corresponding of electron diffraction pattern recorded from the region, showing the nanowire with bead-chain morphology had an amorphous phase structure, (b) EDX spectrum of the nanowire, (c) STEM of SiO_{2+x} nanowire with bead-chain morphology, (d) and (e) were the distributions of oxygen element and silicon element, respectively.

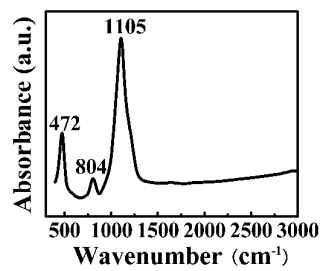


Fig.6 FTIR spectrum of the synthesized SiO_{2+x} nanowires with bead-chain morphology.

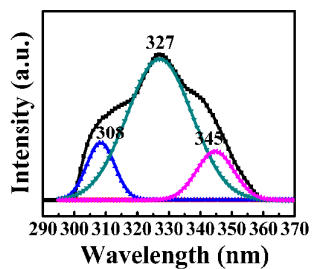


Fig.7 Photoluminescence spectrum of the synthesized SiO_{2-x} nanowires with bead-chain morphology. The spectrum was decomposed to three peaks of 308, 327 and 345 nm.

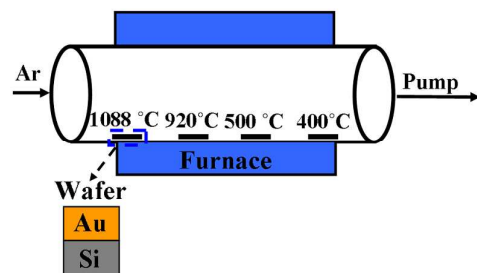


Fig. S1 Schematic of the experimental set up for growth of SiO_{2+x} nanowires in a horizontal tube furnace with different temperatures.

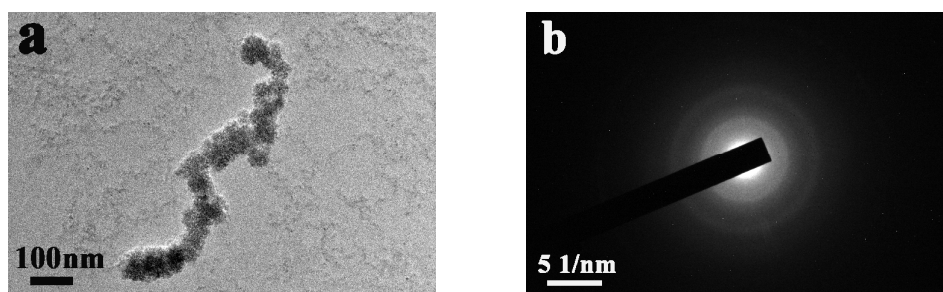


Fig. S2 (a) TEM image of SiO_{2-x} nanowire prepared at lower temperature ($\sim 400^\circ\text{C}$). (b) The corresponding of electron diffraction pattern recorded from the region, showing the nanowire had an amorphous phase structure.

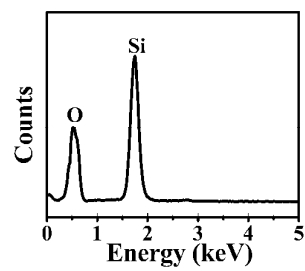


Fig. S3 EDX spectrum of a quartz sample with high purity.

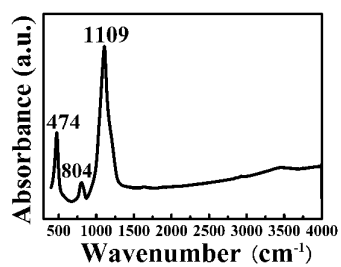


Fig. S4 FTIR spectrum of the SiO_{2-x} nanowires prepared at lower temperature (~ 400°C).

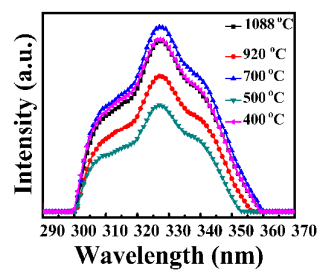


Fig. S5 Photoluminescence spectra of the synthesized SiO_{2+x} nanowires grown at different temperatures.

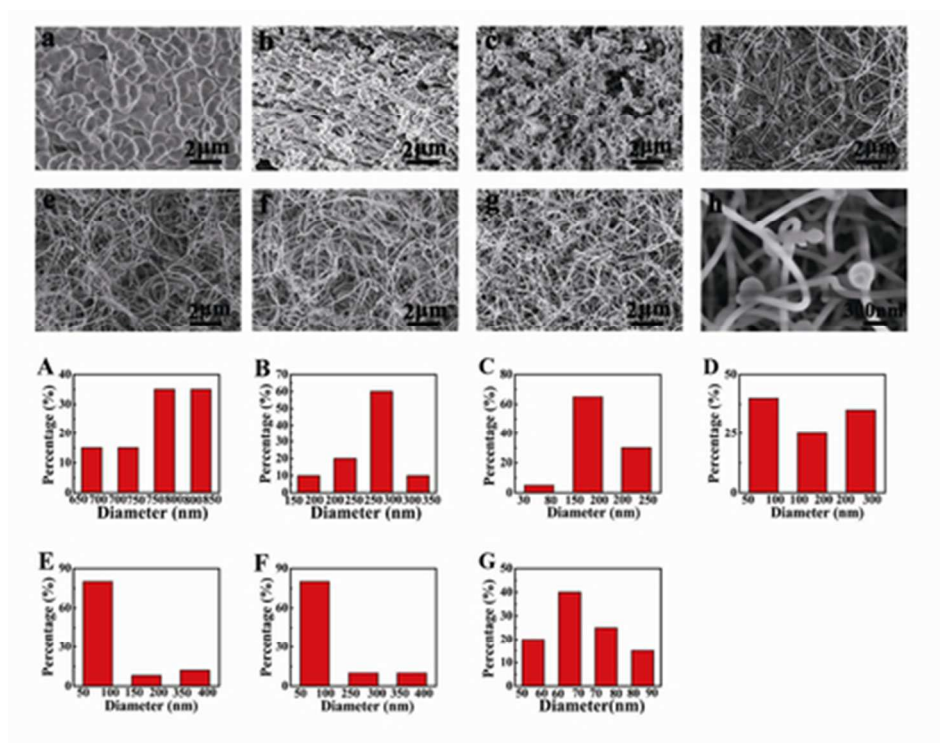


Fig.1 SEM images of SiO₂+x prepared at different temperatures, (a) 1088°C, (b) 920°C, (c) 800°C, (d) 700°C, (e) 600°C, (f) 500°C and (g) 400°C. Image of (h) was the enhanced image of (g). Size histograms of SiO₂+x prepared at the corresponding temperatures were (A), (B), (C), (D), (E), (F) and (G), respectively. The deposition time was set as 30 min and the thickness of Au was ~ 15 nm.
39x31mm (300 x 300 DPI)

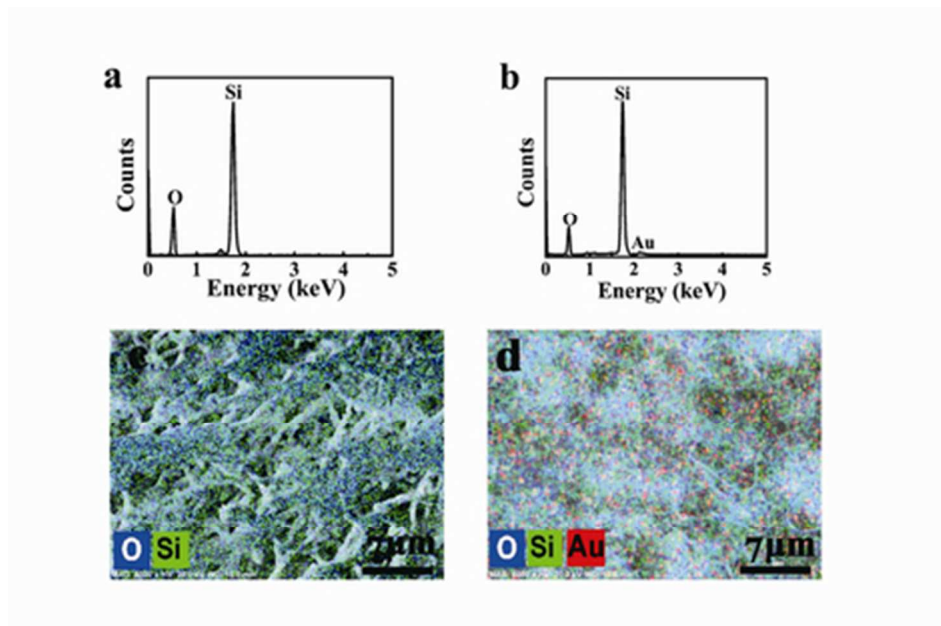


Fig.2 EDX spectra of the nanowires at different temperatures, (a) 1088°C, (b) 400°C. The corresponding EDX mapping scanning spectra of the nanowires at different temperatures, (c) 1088°C, (d) 400°C. For mapping scanning spectra, the color of blue, green and red represented the distributions of oxygen, silicon and gold, respectively. The deposition time was set as 30 min.
39x26mm (300 x 300 DPI)

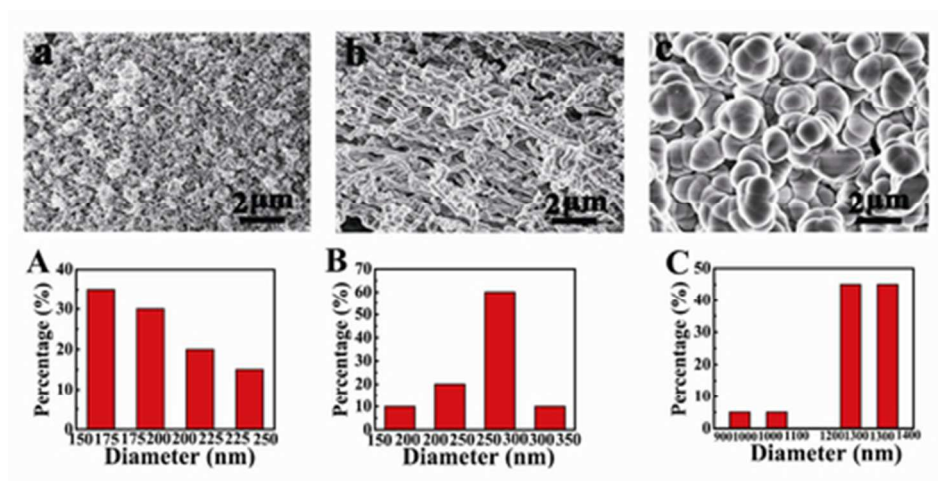


Fig. 3 SEM images of SiO_{2+x} prepared with different deposition time, (a) 15 min, (b) 30 min and (c) 60 min. Size histograms of SiO_{2+x} prepared with different deposition time (A) 15 min, (B) 30 min and (C) 60 min. The temperature was set as $\sim 920^{\circ}\text{C}$.
39x20mm (300 x 300 DPI)

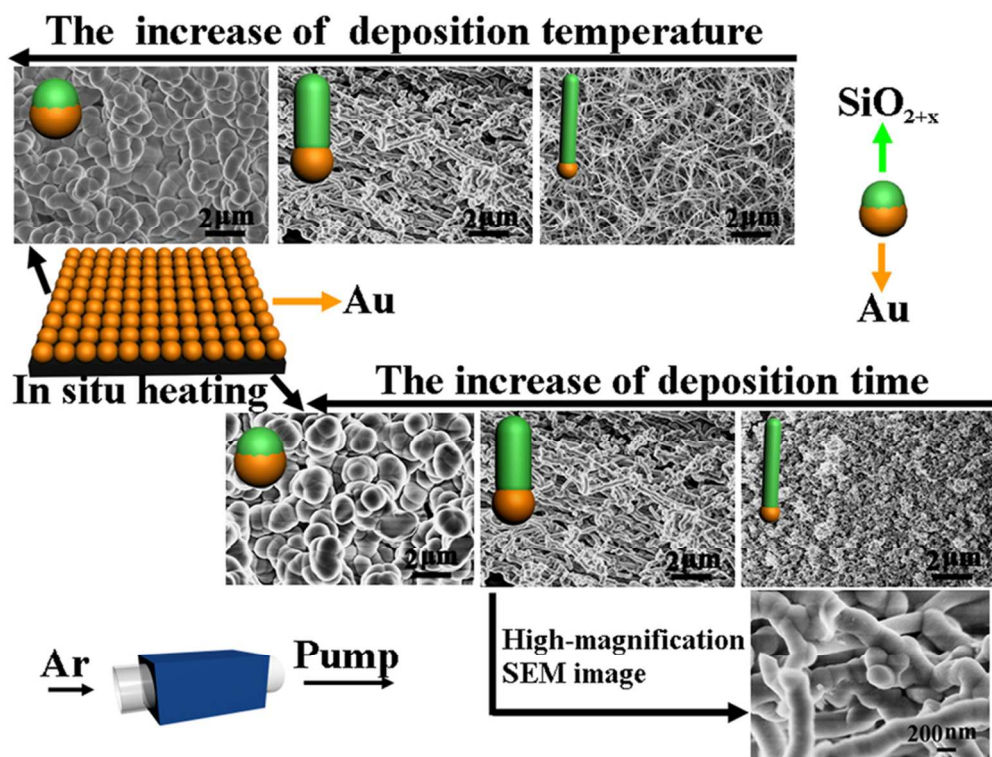


Fig.4 Scheme of a 'dissolution-saturation-precipitation' growth model for SiO_{2+x} nanowires.
40x30mm (600 x 600 DPI)

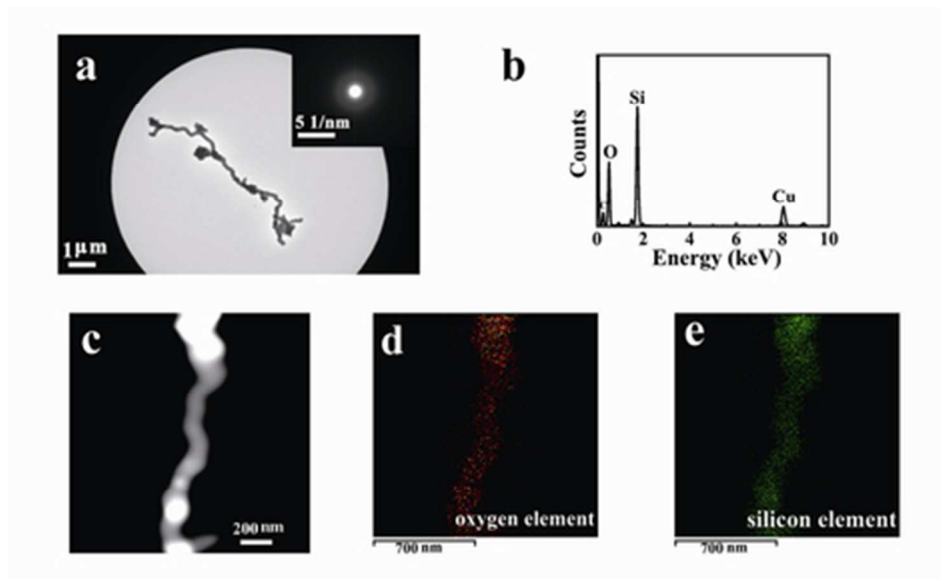


Fig.5 TEM image of (a) SiO₂+x, the insert was the corresponding of electron diffraction pattern recorded from the region, showing the nanowire with bead-chain morphology had an amorphous phase structure, (b) EDX spectrum of the nanowire, (c) STEM of SiO₂+x nanowire with bead-chain morphology, (d) and (e) were the distributions of oxygen element and silicon element, respectively.

39x24mm (300 x 300 DPI)

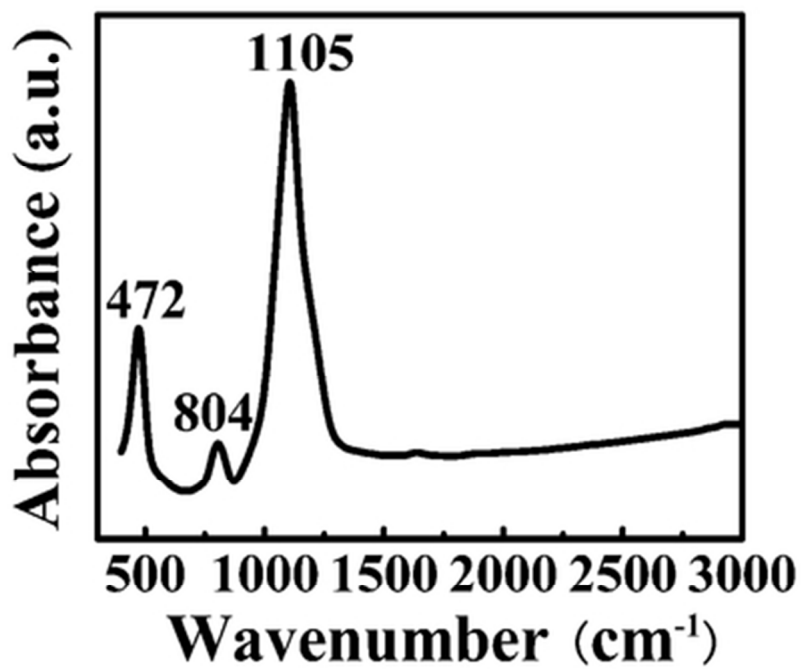


Fig.6 FTIR spectrum of the synthesized SiO₂+x nanowires with bead-chain morphology.
39x30mm (300 x 300 DPI)

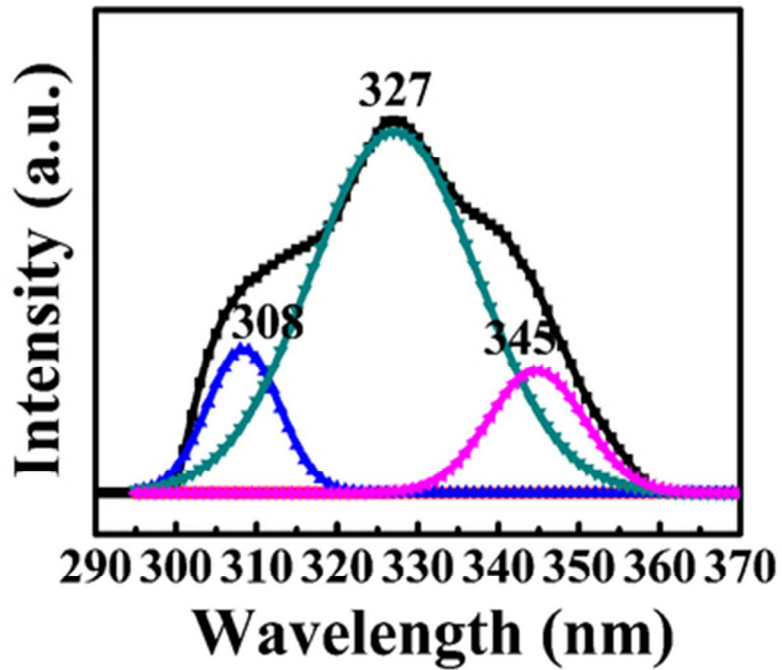


Fig.7 Photoluminescence spectrum of the synthesized SiO_{2+x} nanowires with bead-chain morphology. The spectrum was decomposed to three peaks of 308, 327 and 345 nm.
39x30mm (300 x 300 DPI)